


# Hierarchical simultaneous entanglement swapping for multi-hop quantum communication based on multi-particle entangled states

Guang Yang(杨光), Lei Xing(邢磊), Min Nie(聂敏), Yuan-Hua Liu(刘原华), and Mei-Ling Zhang(张美玲)
**Citation:**Chin. Phys. B, 2021, 30 (**3**): 030301. DOI: 10.1088/1674-1056/abcf3d
Journal homepage: http://cpb.iphy.ac.cn; http://iopscience.iop.org/cpb

**What follows is a list of articles you may be interested in**

---

## Quantum teleportation of particles in an environment

Lu Yang(杨璐), Yu-Chen Liu(刘雨辰), Yan-Song Li(李岩松)
Chin. Phys. B, 2020, 29 (**6**): 060301. DOI: 10.1088/1674-1056/ab84de

## Qubit movement-assisted entanglement swapping

Sare Golkar, Mohammad Kazem Tavassoly, Alireza Nourmandipour
Chin. Phys. B, 2020, 29 (**5**): 050304. DOI: 10.1088/1674-1056/ab7da3

## Quantum dual signature scheme based on coherent states with entanglement swapping

Jia-Li Liu(刘佳丽), Rong-Hua Shi(施荣华), Jin-Jing Shi(石金晶), Ge-Li Lv(吕格莉), Ying Guo(郭迎)
Chin. Phys. B, 2016, 25 (**8**): 080306. DOI: 10.1088/1674-1056/25/8/080306

## Controlled mutual quantum entity authentication using entanglement swapping

Min-Sung Kang, Chang-Ho Hong, Jino Heo, Jong-In Lim, Hyung-Jin Yang
Chin. Phys. B, 2015, 24 (**9**): 090306. DOI: 10.1088/1674-1056/24/9/090306

## An optimized encoding method for secure key distribution by swapping quantum entanglement and its extension

Gao Gan
Chin. Phys. B, 2015, 24 (**8**): 080305. DOI: 10.1088/1674-1056/24/8/080305

---

# Hierarchical simultaneous entanglement swapping for multi-hop quantum communication based on multi-particle entangled states*

Guang Yang(杨光)†, Lei Xing(邢磊), Min Nie(聂敏),
Yuan-Hua Liu(刘原华), and Mei-Ling Zhang(张美玲)

*School of Communications and Information Engineering & School of Artificial Intelligence, Xi'an University of Posts and Telecommunications, Xi'an* 710121, *China*

(Received 10 August 2020; revised manuscript received 8 November 2020; accepted manuscript online 1 December 2020)

Entanglement swapping is a key technology for multi-hop communication based on entanglement in quantum networks. However, the end-to-end delay of the traditional sequential entanglement swapping (SEQES) grows rapidly with the increase of network scale. To solve this problem, we first propose a low-delay multi-particle simultaneous entanglement swapping (SES) scheme to establish the remote four-particle Greenberger–Horne–Zeilinger (GHZ) channel states for the bidirectional teleportation of three-particle GHZ states, in which the intermediate nodes perform Bell state measurements, send the measurement results and the Bell state type to the user node Bob (or Alice) through classical channel simultaneously. Bob (or Alice) only needs to carry out a proper unitary operation according to the information he (or she) has received. Further, we put forward a hierarchical simultaneous entanglement swapping (HSES) scheme to reduce the classical information transmission cost, which is composed of level-1 SES and level-2 SES (schemes). The former is an inner segment SES, and the latter is an inter segments SES. Theoretical analysis and simulation results show the HSES can obtain the optimal performance tradeoff between end-to-end delay and classical cost.

**Keywords:** multi-hop quantum communication, entanglement swapping, teleportation, multi-particle

**PACS:** 03.67.Pp, 03.65.Yz, 03.67.Hk **DOI:** 10.1088/1674-1056/abcf3d

## 1. Introduction

Quantum entanglement plays a critical role in quantum computation and quantum communication, such as quantum teleportation,[1–3] quantum dense coding,[4–6] quantum key distribution,[7–9] and quantum secure direct communication.[10–12] In order to realize multi-user wide area quantum communication, the construction of quantum network has become the focus of attention.[13–15] However, it is difficult to distribute entangled particles between two remote users directly in a quantum network due to the inevitable losses on the quantum channel.

Entanglement swapping (ES) is an important method that can establish the entanglement path between two quantum users who do not share entanglement initially. The ES was first presented in 1993,[16] based on which, various multi-hop quantum communication schemes have been proposed. Cheng *et al.* devised a routing algorithm in wireless quantum networks by using the ES to construct the quantum bridge, and thus realizing the quantum teleportation.[17] Zhou *et al.* proposed a routing strategy for quantum internet, where quantum routers perform ES to establish entanglement connection.[18] The establishing rate of quantum path for point-by-point ES and segmentation ES was analyzed in Ref. [19]. Yu *et al.* proposed a two-end approximation algorithm based on ES in a wireless quantum network.[20] The similarity among the above schemes is that each intermediate node needs to perform ES hop by hop. As a result, the end-to-end time delay of entanglement establishment grows rapidly with the increase of the length and the hop count of a quantum path. We call this type of ES the sequential ES (SEQES).

In order to reduce the establishment delay of entanglement path in a wide area quantum network, Liu *et al.* proposed a three-hop simultaneous ES (SES) scheme, where all intermediate nodes simultaneously conducted Bell state measurements (BSM), and sent the measurement results to the destination node through classical channel.[21] Wang *et al.* proposed a teleportation scheme based on the SES in a multi-hop wireless quantum network.[22] The SES scheme was also applied to the bidirectional quantum teleportation, and the unitary operation to reconstruct the quantum state was obtained by solving the inverse matrix.[23] Gao *et al.* proposed a multi-hop W-state teleportation method based on multi-level binary tree networks with selective receiving nodes, and the nodes at all levels perform quantum measurement and result transmission simultaneously.[24] With the similar ideas, other multi-hop quantum information transmission schemes based on the SES were presented in Refs. [25–27].

However, in the above SES methods, each intermediate

*Project supported by the National Natural Science Foundation of China (Grant No. 61971348), the Scientific Research Program Funded by Shaanxi Provincial Education Department, China (Grant No. 16JK1711), and the Natural Science Foundation Research Project of Shaanxi Province, China (Grant No. 16JQ6033).

†Corresponding author. E-mail: sharon.yg@163.com

© 2021 Chinese Physical Society and IOP Publishing Ltd 

node should send the quantum measurement results to the destination node through classical channel, which would involve the forwarding of the classical information in each classical intermediate node along the classical channel, resulting in a very high classical transmission cost, so they are not suitable for large-scale quantum networks. On the other hand, the existing SES schemes mainly focus on the entanglement swapping of two-particle entangled states. As more powerful resources, multi-particle entangled states have been used in many novel quantum information tasks, including controlled teleportation,[28–30] bidirectional teleportation,[31–33] multi-party quantum secret sharing,[34–36] and multi-party quantum key agreement.[37–39] It is of great value to explore how to realize the multi-particle communication in a multi-hop quantum network rapidly and efficiently.

In this paper, we first put forward an SES scheme to establish the four-particle GHZ entanglement path, which is used to complete the multi-hop bidirectional teleportation of three-particle GHZ states. Further, in order to reduce the classical information cost in SES scheme, we propose a hierarchical SES (HSES) scheme that is composed of level-1 SES and level-2 SES schemes, the former implements the inner segment entanglement swapping and the latter implements the inter segment entanglement swapping. Compared with the basic SES scheme, the HSES obtains a lower classical cost, and still shows a good time delay performance. The rest of the paper is organized as follows. In Section 2, we briefly introduce the process of bidirectional teleportation of three-particle GHZ states. In Section 3, we describe the details of SES scheme to establish the remote entanglement path for the bidirectional teleportation. In Section 4, we propose the HSES scheme. In Section 5, we analyze the performance of SES and HSES. Finally, the conclusions of our work are given in Section 6.

## 2. Bidirectional teleportation of three-particle GHZ states

In this section, we briefly introduce the scheme of the bidirectional teleportation of three-particle Greenberger–Horne–Zeilinger (GHZ) state, and the detailed process can be seen in Ref. [32]. It is supposed that Alice and Bob each have a three-particle GHZ state to be teleported to each other, which has the following form:

$$\begin{aligned}|\psi_1\rangle &= (\alpha_0|000\rangle + \alpha_1|111\rangle)_{A_1A_2A_3},\\ |\psi_2\rangle &= (\beta_0|000\rangle + \beta_1|111\rangle)_{B_1B_2B_3}.\end{aligned} \tag{1}$$

Here, the parameters $\alpha_0$, $\alpha_1$, $\beta_0$, $\beta_1$ satisfy $|\alpha_0|^2+|\alpha_1|^2 = 1$ and $|\beta_0|^2+|\beta_1|^2 = 1$. To accomplish the teleportation, they need to share an eight-particle complex GHZ state $|\omega\rangle$ as the quantum channel in advance, which is shown in Fig. 1. Alice holds the particles $a_1$, $a_2$, $a_3$, $b_4$, while Bob holds the particles $b_1$, $b_2$, $b_3$, $a_4$. $|\omega\rangle$ can be described as the following tensor product of two four-particle GHZ state

$$\begin{aligned}|\omega\rangle = &\frac{1}{\sqrt{2}}(|0000\rangle + |1111\rangle)_{a_1a_2a_3a_4}\\ &\otimes\frac{1}{\sqrt{2}}(|0000\rangle + |1111\rangle)_{b_1b_2b_3b_4}.\end{aligned} \tag{2}$$

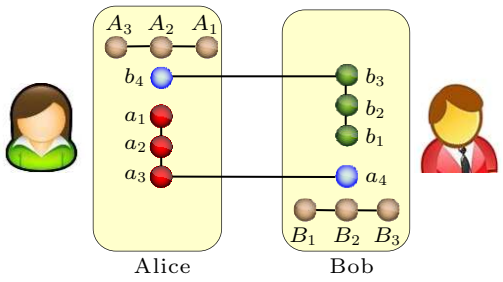



**Fig. 1.** Quantum state preparation for bidirectional teleportation of three-particle GHZ states.

After the quantum states preparation, Alice and Bob carry out the following steps to complete the bidirectional teleportation.

**Step 1** They perform controlled-not (CNOT) operations respectively on particles $A_1$ and $b_4$, $B_1$ and $a_4$, where $A_1$ and $B_1$ are the control particles.

**Step 2** They perform single-qubit $|Z\rangle$-basis measurements on particles $b_4$ and $a_4$ respectively, and perform single-qubit $|X\rangle$-basis measurements on particles $A_2$ and $B_2$ respectively, then they announce the results to each other through classical channel.

**Step 3** They perform single-qubit $|X\rangle$-basis measurements on particles $A_1$ and $B_1$ respectively, then they announce the measurement results thriugh classical channel.

**Step 4** They perform single-qubit $|X\rangle$-basis measurements on particles $A_3$ and $B_3$ respectively, then they announce the measurement results through classical channel.

**Step 5** They perform proper three-particle unitary operations on particles $a_1$, $a_2$, $a_3$ and $b_1$, $b_2$, $b_3$ according to the measurement results in Step 2, Step 3, and Step 4, then the bidirectional teleportation is finished.

For example, if the measurement results in Step 2, Step 3, Step 4 are $|++00\rangle_{A_2B_2b_4a_4}$, $|{+}{+}\rangle_{A_1B_1}$, $|{+}{+}\rangle_{A_3B_3}$, then the states of particles $b_1$, $b_2$, $b_3$ and $a_1$, $a_2$, $a_3$ turn into

$$\begin{aligned}&|\chi\rangle_{b_1b_2b_3a_1a_2a_3}\\ &= (\alpha_0\beta_0|000000\rangle + \alpha_0\beta_1|000111\rangle\\ &\quad + \alpha_1\beta_0|111000\rangle + \alpha_1\beta_1|111111\rangle)_{b_1b_2b_3a_1a_2a_3}\\ &= (\alpha_0|000\rangle + \alpha_1|111\rangle)_{b_1b_2b_3}\\ &\quad \otimes(\beta_0|000\rangle + \beta_1|111\rangle)_{a_1a_2a_3}.\end{aligned} \tag{3}$$

In this case, the three-particle unitary operations of Alice and Bob are $I_{a_1}\otimes I_{a_2}\otimes I_{a_3}$ and $I_{b_1}\otimes I_{b_2}\otimes I_{b_3}$. After the unitary operations, Alice reconstructs the initial state $|\psi_2\rangle$ on her particles

$a_1$, $a_2$, and $a_3$, and Bob reconstructs the initial state $|\psi_1\rangle$ on his particles $b_1$, $b_2$, and $b_3$. The bidirectional quantum teleportation of three-qubit GHZ states is completed successfully. The unitary operations can be calculated when other measurement results are obtained.

The above scheme can be extended to realizing the bidirectional teleportation of $n$-particle GHZ states with a $2N$-particle ($N = n+1$) complex GHZ channel state.

## 3. SES for multi-hop bidirectional teleportation of three-particle GHZ states

### 3.1. Basic scheme of SES

In a quantum network, there is usually no direct quantum channel between two remote users. In order to realize the bidirectional teleportation in Section 2 in a multi-hop quantum network, we propose an SES scheme that can establish the remote four-particle GHZ entanglement path. At first, we consider a scenario of three-hop SES illustrated in Fig. 2. The complete process consists of the following steps.

**Step 1** Entanglement state preparation and entanglement distribution

Alice prepares a four-particle GHZ state $|\omega_A\rangle = (1/\sqrt{2})(|0000\rangle + |1111\rangle)_{a_1a_2a_3a_4}$, then she holds the particles $a_1$, $a_2$, $a_3$ and distributes particle $a_4$ to the intermediate node $R_1$. Bob prepares a four-particle GHZ state $|\omega_B\rangle = (1/\sqrt{2})(|0000\rangle + |1111\rangle)_{b_1b_2b_3b_4}$, then he holds the particles $b_1$, $b_2$, $b_3$ and distributes particle $b_4$ to the intermediate node $R_2$. Node $R_1$ prepares two Bell states $|\phi_{R_{1A}}\rangle = (1/\sqrt{2})(|00\rangle + |11\rangle)_{a_5a_6}$ and $|\phi_{R_{1B}}\rangle = (1/\sqrt{2})(|00\rangle + |11\rangle)_{b_7b_8}$, then he distributes particle $a_6$ to $R_2$ and distributes particle $b_8$ to Alice. Node $R_2$ prepares two Bell states $|\phi_{R_{2A}}\rangle = (1/\sqrt{2})(|00\rangle + |11\rangle)_{a_7a_8}$ and $|\phi_{R_{2B}}\rangle = (1/\sqrt{2})(|00\rangle + |11\rangle)_{b_5b_6}$, then he distributes particle $a_8$ to Bob and distributes particle $b_6$ to node $R_1$.

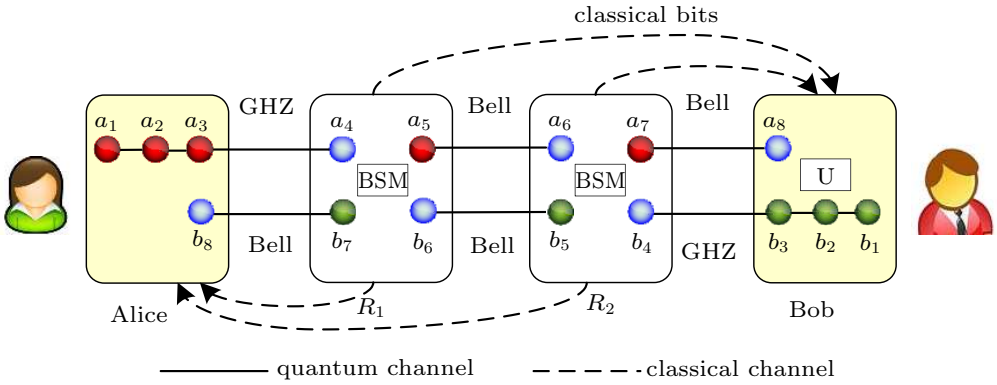



**Fig. 2.** Three-hop simultaneous entanglement swapping of GHZ channel state.

In Fig. 2, the particles $a_1$, $a_2$, $a_3$, $a_4$, $a_5$, $a_6$, $a_7$, and $a_8$ constitute one channel for the bidirectional teleportation, and we call it channel $A$. The particles $b_1$, $b_2$, $b_3$, $b_4$, $b_5$, $b_6$, $b_7$, and $b_8$ constitute the other channel, and we call it channel $B$. We take channel $A$ for example. After the particles distribution, the total state of particles $a_1$, $a_2$, $a_3$, $a_4$, $a_5$, $a_6$, $a_7$, and $a_8$ is expressed as

$$\begin{aligned}
&|\omega_{\mathrm{TA}-3}\rangle \\
&= \frac{1}{\sqrt{2}}(|0000\rangle + |1111\rangle)_{a_1a_2a_3a_4} \\
&\quad \otimes \frac{1}{\sqrt{2}}(|00\rangle + |11\rangle)_{a_5a_6} \otimes \frac{1}{\sqrt{2}}(|00\rangle + |11\rangle)_{a_7a_8} \\
&= \frac{1}{2}(|000000\rangle + |000011\rangle + |111100\rangle \\
&\quad + |111100\rangle)_{a_1a_2a_3a_4a_5a_6} \otimes \frac{1}{\sqrt{2}}(|00\rangle + |11\rangle)_{a_7a_8} \\
&= \frac{1}{2}(|0000\rangle_{a_1a_2a_3a_6}|00\rangle_{a_4a_5} + |0001\rangle_{a_1a_2a_3a_6}|01\rangle_{a_4a_5} \\
&\quad + |1110\rangle_{a_1a_2a_3a_6}|10\rangle_{a_4a_5} + |1111\rangle_{a_1a_2a_3a_6}|11\rangle_{a_4a_5}) \\
&\quad \otimes \frac{1}{\sqrt{2}}(|00\rangle + |11\rangle)_{a_7a_8}. \qquad (4)
\end{aligned}$$

Using $|\phi^{\pm}\rangle = (1/\sqrt{2})(|00\rangle \pm |11\rangle)$ and $|\phi^{\pm}\rangle = (1/\sqrt{2})(|01\rangle \pm |10\rangle)$, equation (4) can be rewritten as

$$\begin{aligned}
&|\omega_{\mathrm{TA}-3}\rangle \\
&= \frac{1}{2\sqrt{2}}[(|0000\rangle + |1111\rangle)_{a_1a_2a_3a_6}|\phi^+\rangle_{a_4a_5}|\phi^+\rangle_{a_7a_8} \\
&\quad + (|0000\rangle - |1111\rangle)_{a_1a_2a_3a_6}|\phi^-\rangle_{a_4a_5}|\phi^+\rangle_{a_7a_8} \\
&\quad + (|0001\rangle + |1110\rangle)_{a_1a_2a_3a_6}|\varphi^+\rangle_{a_4a_5}|\phi^+\rangle_{a_7a_8} \\
&\quad + (|0001\rangle - |1110\rangle)_{a_1a_2a_3a_6}|\varphi^-\rangle_{a_4a_5}|\phi^+\rangle_{a_7a_8}]. \qquad (5)
\end{aligned}$$

Defining $|\omega_1\rangle = (1/\sqrt{2})(|0000\rangle + |1111\rangle)$ as a standard four-particle GHZ state, we can obtain other four-particle GHZ states with proper unitary operations on $|\omega_1\rangle$:

$$\begin{aligned}
|\omega_1\rangle &= \frac{1}{\sqrt{2}}(|0000\rangle + |1111\rangle) = U_1|\omega_1\rangle = I\otimes I\otimes I\otimes I|\omega_1\rangle, \\
|\omega_2\rangle &= \frac{1}{\sqrt{2}}(|0000\rangle - |1111\rangle) = U_2|\omega_1\rangle = I\otimes I\otimes I\otimes Z|\omega_1\rangle, \\
|\omega_3\rangle &= \frac{1}{\sqrt{2}}(|0001\rangle + |1110\rangle) = U_3|\omega_1\rangle = I\otimes I\otimes I\otimes X|\omega_1\rangle, \\
|\omega_4\rangle &= \frac{1}{\sqrt{2}}(|0001\rangle - |1110\rangle) = U_4|\omega_1\rangle
\end{aligned}$$

$$= I\otimes I\otimes I\otimes ZX\,|\omega_1\rangle\,. \quad (6)$$

Using Eq. (6), we can rewrite Eq. (5) as

$$\begin{aligned}|\omega_{\mathrm{TA}-3}\rangle \;=\; & \frac{1}{2}(U_1\,|\omega_1\rangle_{a_1a_2a_3a_6}\,|\phi^+\rangle_{a_4a_5}\,|\phi^+\rangle_{a_7a_8}\\ & +U_2\,|\omega_1\rangle_{a_1a_2a_3a_6}\,|\phi^-\rangle_{a_4a_5}\,|\phi^+\rangle_{a_7a_8}\\ & +U_3\,|\omega_1\rangle_{a_1a_2a_3a_6}\,|\varphi^+\rangle_{a_4a_5}\,|\phi^+\rangle_{a_7a_8}\\ & +U_4\,|\omega_1\rangle_{a_1a_2a_3a_6}\,|\varphi^-\rangle_{a_4a_5}\,|\phi^+\rangle_{a_7a_8}).\end{aligned} \quad (7)$$

Equation (7) can be expanded into the following form:

$$\begin{aligned}|\omega_{\mathrm{TA}-3}\rangle \;=\; & \frac{1}{4}[(|\omega_1\rangle_{a_1a_2a_3a_8}\,U_1^p\,|\phi^+\rangle_{a_6a_7}\\ & +|\omega_2\rangle_{a_1a_2a_3a_8}\,U_1^p\,|\phi^-\rangle_{a_6a_7}\\ & +|\omega_3\rangle_{a_1a_2a_3a_8}\,U_1^p\,|\varphi^+\rangle_{a_6a_7}\\ & +|\omega_4\rangle_{a_1a_2a_3a_8}\,U_1^p\,|\varphi^-\rangle_{a_6a_7})\,|\phi^+\rangle_{a_4a_5}\\ & +(|\omega_1\rangle_{a_1a_2a_3a_8}\,U_2^p\,|\phi^+\rangle_{a_6a_7}\\ & +|\omega_2\rangle_{a_1a_2a_3a_8}\,U_2^p\,|\phi^-\rangle_{a_6a_7}\\ & +|\omega_3\rangle_{a_1a_2a_3a_8}\,U_2^p\,|\varphi^+\rangle_{a_6a_7}\\ & +|\omega_4\rangle_{a_1a_2a_3a_8}\,U_2^p\,|\varphi^-\rangle_{a_6a_7})\,|\phi^-\rangle_{a_4a_5}\\ & +(|\omega_1\rangle_{a_1a_2a_3a_8}\,U_3^p\,|\phi^+\rangle_{a_6a_7}\\ & +|\omega_2\rangle_{a_1a_2a_3a_8}\,U_3^p\,|\phi^-\rangle_{a_6a_7}\\ & +|\omega_3\rangle_{a_1a_2a_3a_8}\,U_3^p\,|\varphi^+\rangle_{a_6a_7}\\ & +|\omega_4\rangle_{a_1a_2a_3a_8}\,U_3^p\,|\varphi^-\rangle_{a_6a_7})\,|\varphi^+\rangle_{a_4a_5}\\ & +(|\omega_1\rangle_{a_1a_2a_3a_8}\,U_4^p\,|\phi^+\rangle_{a_6a_7}\\ & +|\omega_2\rangle_{a_1a_2a_3a_8}\,U_4^p\,|\phi^-\rangle_{a_6a_7}\\ & +|\omega_3\rangle_{a_1a_2a_3a_8}\,U_4^p\,|\varphi^+\rangle_{a_6a_7}\\ & +|\omega_4\rangle_{a_1a_2a_3a_8}\,U_4^p\,|\varphi^-\rangle_{a_6a_7})\,|\varphi^-\rangle_{a_4a_5}].\end{aligned} \quad (8)$$

In Eq. (7), $U_i^p$ $(i=1,2,3,4)$ denotes a two-particle unitary operation which can de described as $U_1^p = I\otimes I$, $U_2^p = Z\otimes I$, $U_3^p = X\otimes I$, $U_4^p = ZX\otimes I$.

**Step 2** Bell state measurements and unitary operations

After the entanglement distribution, the intermediate nodes $R_1$ and $R_2$ perform Bell state measurements (BSMs) on their particles $a_4$, $a_5$ and $a_6$, $a_7$ simultaneously, then they obtain one of the four results $|\phi^+\rangle$, $|\phi^-\rangle$, $|\varphi^+\rangle$ and $|\varphi^-\rangle$ with equal probability. Nodes $R_1$ and $R_2$ encode the four measurement results into two-bit classical codes 00, 01, 10 or 11, then they send the two-bit codes through classical channel to Bob simultaneously. Bob carries out an appropriate unitary operation on his particle $a_8$ according to the classical codes he has received, after which a standard four-particle GHZ state $|\omega_1\rangle$ can be established on particles $a_1$, $a_2$, $a_3$, and $a_8$ between Alice and Bob. The unitary operations can be derived from Eq. (8), which are shown in Table 1. With a similar process, another standard four-particle GHZ state can be established on particles $b_1$, $b_2$, $b_3$, and $b_8$ in channel B.

For example, when the measurement results of $a_4$, $a_5$ and $a_6$, $a_7$ are $|\phi^-\rangle_{a_4a_5}$ and $U_2^p\,|\phi^+\rangle_{a_6a_7}$, then the classical codes are 0101, so the unitary operation on $a_8$ is $I$-gate according to Table 1.

**Table 1.** Unitary operations of Bob in three-hop SES.

| Measurement results of $a_4$, $a_5$, and $a_6$, $a_7$ | Quantum state of $a_1$, $a_2$, $a_3$, $a_8$ | Bob's operation on particle $a_8$ |
|---|---|---|
| 0000, 0101<br>1010, 1111 | $(1/\sqrt{2})(\|0000\rangle+\|1111\rangle)$ | $I$-gate |
| 0001, 0100<br>1011, 1110 | $(1/\sqrt{2})(\|0000\rangle-\|1111\rangle)$ | $Z$-gate |
| 0010, 0111<br>1000, 1101 | $(1/\sqrt{2})(\|0001\rangle+\|1110\rangle)$ | $X$-gate |
| 0011, 0110<br>1001, 1100 | $(1/\sqrt{2})(\|0001\rangle-\|1110\rangle)$ | $ZX$-gate |

The scheme above can be easily extended to the case of $N$-hop multi-particle entanglement swapping. In the $N$-hop scenario, there are $N-1$ intermediate nodes numbered as $R_1$, $R_2$, …, $R_{N-1}$ between Alice and Bob. For the convenience of description, the particles held by $R_i$ in channel A are denoted as $R_{i1}$ and $R_{i2}$ respectively, and the two-bit result code of BSM on $R_{i1}$ and $R_{i2}$ is referred to as $MR_{i1}MR_{i2}$, then the unitary operations of Bob can be obtained from Table 2.

**Table 2.** Unitary operations of Bob in $N$-hop SES.

| Measurement results of $R_1$ to $R_{N-1}$ | Bob's operation on his particle |
|---|---|
| $\overline{\oplus_{i=1}^{N-1}MR_{i1}}\cdot\overline{\oplus_{i=1}^{N-1}MR_{i2}}=1$ | $I$-gate |
| $\overline{\oplus_{i=1}^{N-1}MR_{i1}}\cdot\oplus_{i=1}^{N-1}MR_{i2}=1$ | $Z$-gate |
| $\oplus_{i=1}^{N-1}MR_{i1}\cdot\overline{\oplus_{i=1}^{N-1}MR_{i2}}=1$ | $X$-gate |
| $\oplus_{i=1}^{N-1}MR_{i1}\cdot\oplus_{i=1}^{N-1}MR_{i2}=1$ | $ZX$-gate |

### 3.2. Modified unitary operations in arbitrary Bell states

In practice, the Bell state generated by each intermediate node is not always the state $|\phi^+\rangle$, it may be one of the four Bell states $|\phi^+\rangle$, $|\phi^-\rangle$, $|\varphi^+\rangle$, $|\varphi^-\rangle$. Therefore, in addition to sending the BSM results to Bob, the intermediate node also needs to send the type of the Bell state generated by itself. It can be proved that the final unitary operation that Bob adopts is related to the number of different types of Bell states generated by all intermediate nodes, while it is irrelevant to the order of the Bell states in the multi-hop quantum path. As a result, Bob needs to count the number of the four types of Bell states and calculate a modified unitary operation which is shown in Table 3.

The four-bit sequence code in Table 3 denotes the mod 2 result of the count value of the four types Bell states $|\phi^+\rangle$, $|\phi^-\rangle$, $|\varphi^+\rangle$, and $|\varphi^-\rangle$. Bob obtains the basic unitary operation

from Table 1 or Table 2, and obtains the modified unitary operation from Table 3, then he obtains the final unitary operation by multiplying the two operations.

**Table 3.** Modified unitary operations.

| Mod 2 results of four types of Bell states | Bob's modified operation on his particle |
|---|---|
| 0000 0111 1000 1111 | $I$-gate |
| 0011 0100 1011 1100 | $Z$-gate |
| 0010 0101 1010 1101 | $X$-gate |
| 0001 0110 1001 1110 | $ZX$-gate |

Take the three-hop SES in Fig. 2 for example. Suppose that the Bell states generated by $R_1$ and $R_2$ are $|\phi^+\rangle_{a_5a_6}$ and $|\phi^+\rangle_{a_7a_8}$, then the count value of the $|\phi^+\rangle$ states will be two and the count value of other Bell states is zero, thus Bob obtains a mod 2 result 0000. According to Table 3, Bob obtains the modified unitary operation $I$-gate. Suppose that the Bell states generated by $R_1$ and $R_2$ are $|\phi^+\rangle_{a_5a_6}$ and $|\phi^-\rangle_{a_7a_8}$, then Bob will obtain a mod 2 result 1100, so he obtains the modified unitary operation $Z$-gate.

## 4. The hierarchical simultaneous entanglement swapping

In the SES scheme in Section 3, each intermediate node needs to send the BSM results and the type of the Bell state to Bob through the classical channel, which will lead to considerable classical information transmission costs. In order to solve this problem, we propose a hierarchical SES (HSES) scheme in this section, and the basic process of it is shown in Fig. 3.

In the HSES, the intermediate nodes on the quantum path are divided into several segments according to the scale of the network. The end node of each segment is represented in gray in Fig. 3. A complete HSES process includes the following steps.

**Step 1** Entanglement state preparation and entanglement distribution

This step includes a similar process to the Step 1 of basic SES described in Subsection 3.1, except the fact that the end nodes must generate Bell state $|\phi^+\rangle$, while other intermediate nodes can generate arbitrary Bell states.

**Step 2** Level-one simultaneous entanglement swapping

Level-one SES refers to the entanglement swapping in each segment, and it is carried out concurrently in all segments. With a similar process to that in Subsection 3.1, each intermediate node (except the end node) in a segment performs the BSM on the two particles in each intermediate node's hand, then transmits the measurement result and the type of the Bell state prepared in Step 1 to the end node through the classical channel. After that, the end node calculates the unitary operation according to Tables 2 and 3, and performs the unitary operation on the particle the end node holds. When the level-one SES is finished, the standard four-particle GHZ state $|\omega_1\rangle$ will be established between the end node and the source node in the first segment, while the standard Bell state $|\phi^+\rangle$ will be established between the adjacent end nodes in the remaining segments (*e.g.* the end nodes in segment $i$ and segment $i+1$), which can be seen in Fig. 4. Then, level-two SES will be performed.

**Step 3** Level-two simultaneous entanglement swapping

Level-two SES refers to the entanglement swapping between segments. The end node of each segment performs the BSM on his two particles, and sends the measurement result to Bob concurrently. In this stage, since the end node of the corresponding segment has adjusted the Bell state to $|\phi^+\rangle$, it is not required to transmit the Bell state type information through the classical channel. After receiving all of the measurement results, Bob calculates the unitary operation according to Table 2, and performs the unitary operation on the particle he holds, so as to establish the standard four-particle GHZ state $|\omega_1\rangle$ with Alice.

Due to the fact that the transmission of the BSM results and the Bell state types is limited to a smaller scope in level-one swapping, and the Bell state types need not to be transmitted in level-two swapping, the classical information cost can be significantly reduced by using the HSES.

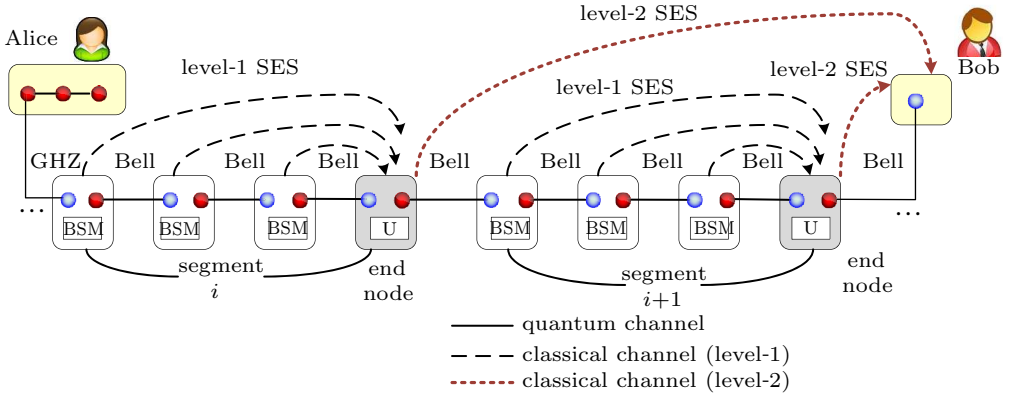



**Fig. 3.** Hierarchical simultaneous entanglement swapping.

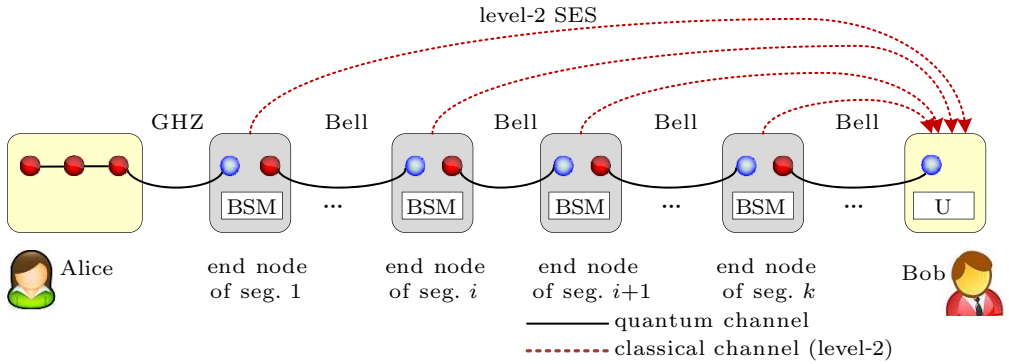



**Fig. 4.** Level-two simultaneous entanglement swapping. Abbreviation "seg." = segment.

## 5. Analysis and discussion

### 5.1. End-to-end time delay of entanglement swapping

Suppose that there are $N$ hops in an entanglement swapping path between Alice and Bob, which means that the total number of the intermediate nodes is $N-1$.

In the SEQES, each intermediate node needs to perform the unitary operation, BSM, and classical information transmission in sequence. The total end-to-end time delay $D_{\text{seq}}$ of SEQES can be calculated from the following formula

$$D_{\text{seq}} = D_{\text{d}} + \sum_{i=1}^{N-1} [H_i(D_{\text{c}} + L_{\text{mt}}/R_{\text{c}} + D_{\text{pro}}) + D_{\text{m}} + D_{\text{u}}]. \quad (9)$$

Here, $D_{\text{d}}$ is the average entanglement distribution time in one quantum hop between two adjacent quantum nodes, $D_{\text{c}}$ is the average information transmission delay in one classical hop, $H_i$ is the number of the classical hops between the $i$-th intermediate node and the $(i+1)$-th intermediate node, $L_{\text{mt}}$ is the total length of the classical packet which carries the information about the BSM result and Bell-state type, $R_{\text{c}}$ is the transmission rate of classical information, $D_{\text{pro}}$ is the average processing time for a classical packet, $D_{\text{m}}$ is the average time of a BSM, and $D_{\text{u}}$ is the average time of a unitary operation.

In the SES described in Section 3, after the entanglement distribution and the BSM, each intermediate node sends the classical information to Bob simultaneously. The delay of classical information transmission depends on the maximum delay from each intermediate node to Bob. Therefore, the total end-to-end time delay $D_{\text{s}}$ of SES can be calculated from

$$D_{\text{s}} = D_{\text{d}} + (D_{\text{c}} + D_{\text{pro}} + L_{\text{mt}}/R_{\text{c}})H_{\max} + D_{\text{m}} + D_{\text{u}}, \quad (10)$$

where $H_{\max}$ represents the maximum classical hop count between each intermediate node and Bob.

In the HSES described in Section 4, after the entanglement distribution, the delay of level-one SES depends on the maximum entanglement swapping delay of all segments, and the delay of level-two SES depends on the maximum delay from each end node to Bob. Therefore, the total end-to-end time delay $D_{\text{hs}}$ of HSES can be calculated from

$$\begin{aligned} D_{\text{hs}} = {} & D_{\text{d}} + H_{\max-\text{s}}(D_{\text{c}} + D_{\text{pro}} + L_{\text{mt}}/R_{\text{c}}) \\ & + H_{\max-\text{en}}(D_{\text{c}} + D_{\text{pro}} + L_{\text{m}}/R_{\text{c}}) + 2D_{\text{m}} + 2D_{\text{u}}. \end{aligned} \quad (11)$$

In Eq. (11), $H_{\max-\text{s}}$ represents the maximum classical hop count between the first intermediate node and the end node in all segments, $H_{\max-\text{en}}$ represents the maximum classical hop count between each end node and Bob, $L_{\text{m}}$ represents the length of the classical packet which carries the BSM result. Owing to the fact that the entanglement states between the adjacent intermediate nodes have been adjusted to standard $|\phi^+\rangle$ in level-one SES, it is not required to transmit Bell state type information.

In the following simulation, it is assumed that the propagation rate of photon in the air is $2.996 \times 10^5$ km, $D_{\text{m}}$ is 100 ns, $D_{\text{u}}$ is 50 ns, $D_{\text{pro}}$ is 20 ns, and $R_{\text{c}}$ is 100 Mbit/s. The lengths of $L_{\text{mt}}$ and $L_{\text{m}}$ are both taken to be 512 bits due to the fact that the classical code of BSM result and the Bell-state type must be carried in a standard data packet, then this packet should be encapsulated into MAC frame, and the length of the shortest MAC frame is 512 bits.

The end-to-end time delay of SEQES, SES, and HSES varying with the number of the intermediate nodes are shown in Fig. 5. Here, the length of one quantum hop is taken to be 10 km, and the number of the intermediate nodes of one segment of HSES is taken to be 4. We can see that the time delays of the three schemes all increase with the number of the intermediate nodes increasing, and the delay of SEQES is much higher than that of SES and HSES. This is because an intermediate node must perform the required processes one after another in SEQES, yet in SES and HSES, intermediate nodes can perform these processes simultaneously. Meanwhile, the time delay of HSES is slightly higher than that of SES.

Suppose that the distance from Alice to Bob is given, the end-to-end delay of SEQES, SES, and HSES are given in Fig. 6. when the per-hop length between two adjacent intermediate nodes is separately 5 km, 10 km, and 20 km. The number of the intermediate nodes in one segment of HSES

is taken to be 4 when the per-hop length is separately 10 km and 20 km, and it is taken to be 8 when the per-hop length is 5 km. It can be seen that the delay of SEQES is still higher than that of HSES, while the delay of HSES is slightly higher than that of SES. When the per-hop length is 20 km, SEQES, SES, and HSES all obtain the lowest time delays, and they obtain the highest time delays when the per-hop length is 5 km. Obviously, a shorter per-hop length means a larger number of intermediate nodes when the distance from Alice to Bob is given. In other words, it will lead the end-to-end delay to increase when too many intermediate nodes are placed between Alice and Bob. However, when the number of the intermediate nodes decreases, the length between adjacent nodes will increase, which brings about the considerable decoherence and noise in quantum channel. As a result, it is very important to determine the per-hop length appropriately.

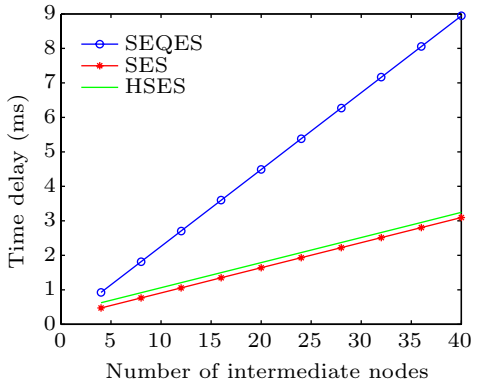



**Fig. 5.** Time delay *versus* number of intermediate nodes for SEQES, SES, and HSES.

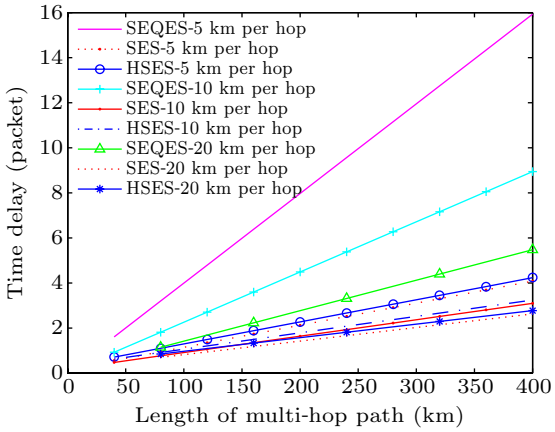



**Fig. 6.** Time delay *versus* length of nulti-hop path for SEQES and HSES in the case of different per-hop lengths.

### 5.2. Classical information cost of entanglement swapping

In the SEQES, each intermediate node needs to send the classical information about the BSM results and the type of the Bell state to the next intermediate node. The overall classical information cost of SEQES is

$$C_{\text{seq}} = \sum_{i=1}^{N-1} L_{\text{mt}} H_i. \tag{12}$$

In the SES described in Section 3, each intermediate node needs to send classical information to Bob, so the overall classical information cost can be calculated from

$$C_{\text{s}} = \sum_{i=1}^{N-1} L_{\text{mt}} H_i^{\text{d}}, \tag{13}$$

where $H_i^{\text{d}}$ denotes the number of the classical hops between the $i$-th intermediate node and the user node Bob.

In the HSES described in Section 4, the overall classical information cost is

$$C_{\text{hs}} = \sum_{k=1}^{N_{\text{s}}} \sum_{j=1}^{P_k-1} L_{\text{mt}} H_{kj}^{\text{s}} + \sum_{k=1}^{N_{\text{s}}} L_{\text{m}} H_k^{\text{d}}. \tag{14}$$

Here, $N_{\text{s}}$ is the total number of the segments, $P_k$ is the total number of the intermediate nodes in segment $k$, $H_{kj}^{\text{s}}$ denotes the number of the classical hops between the $j$-th intermediate node and the end node in segment $k$, $H_k^{\text{d}}$ represents the number of the classical hops between the end node of segment $k$ and Bob, and $P_k$ satisfies

$$\sum_{k=1}^{N_{\text{s}}} P_k = N - 1. \tag{15}$$

In the following simulation, we use the packet as the unit of the classical cost due to the fact that the classical information should be carried in a data packet which is encapsulated in Mac frame.

The classical costs of SEQES, SES, and HSES varying with the increase of the number of intermediate nodes are shown in Fig. 7. Here, we assume that the classical hop count between two adjacent intermediate nodes is 1, and we take 4 intermediate nodes in one segment in HSES. It can be seen that the classical cost of SES is the highest in the three schemes, while the classical cost of HSES is much lower than that of SES, and the classical cost of SEQES is the lowest.

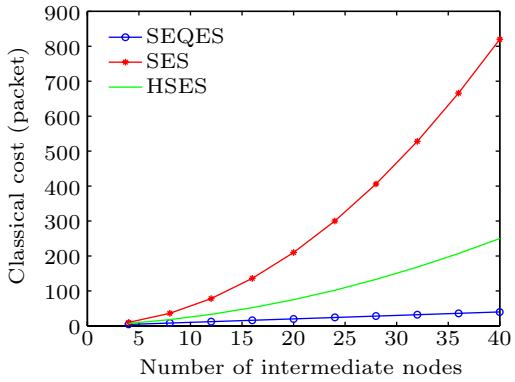



**Fig. 7.** Classical costs *versus* number of intermediate nodes for SEQES, SES, and HSES.

Suppose that the total number of the intermediate nodes between Alice and Bob is given, figure 8 shows the classical costs of HSES when the numbers of intermediate nodes are 1, 4, 8, and 16 in one segment. It can be seen that when there is 1 node in a segment, which is equal to the scenario of SES, the

classical cost is the highest; and the cost is the lowest when there are 8 nodes in a segment, while the cost in the case of 4 nodes and 16 nodes are a bit higher. Therefore, a larger node number in a segment does not always bring lower cost because it leads to a higher cost of level-one SES. Consequently, it is very important to give an appropriate segmentation method, thereby obtaining an optimal classical cost.

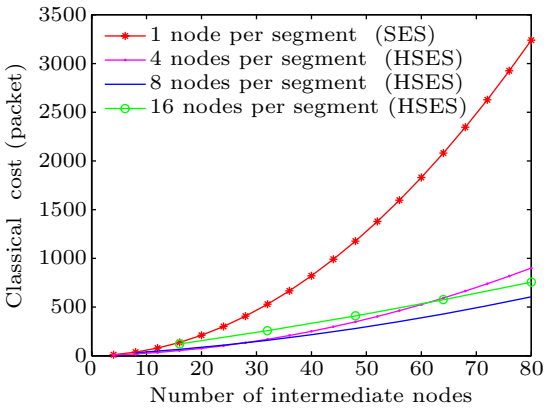



**Fig. 8.** Classical costs *versus* number of intermediate nodes for HSES with different numbers of nodes in one segment.

Assume that the total number of the intermediate nodes is given in HSES, figure 9 shows the comparison among the classical costs when the classical hop counts between two adjacent intermediate nodes are different. The number of the intermediate nodes in one segment is taken to be 4. From Fig. 9. we can see that the classical cost is the highest when the classical hop count is 3, while it is the lowest when the classical hop count is 1. Due to the fact that each classical node in one classical hop must store and forward the classical packets, the classical cost rises with the increase of the classical hop count.

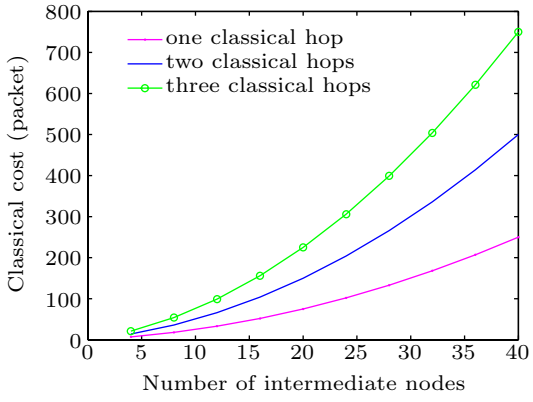



**Fig. 9.** Classical costs *versus* number of intermediate nodes for HSES with different classical hops between adjacent quantum intermediate nodes.

### 5.3. Discussion on challenge of Bell-state measurement

A significant challenge in multi-hop quantum entanglement swapping is the need of performing complete BSM, which also plays a critical role in other quantum information tasks, such as quantum teleportation and quantum dense coding. However, traditional BSM schemes with linear optics can only distinguish two of the four Bell states unambiguously, thus the success probability is no more than 50%.[40–42]

Although the complete BSM schemes with nonlinear optical elements have been presented, such as the cross-Kerr nonlinearity and the quantum-dot system,[43–45] they are still hard to put into practical application. In the past few years, researchers have been working on achieving a complete BSM with linear optics, and several improved schemes have been proposed, such as the use of auxiliary particles,[46,47] compression operation,[48] and ancillary degree of freedom (DOF).[49–52] Grice proposed a complete BSM by using the linear optical elements with the addition of ancillary entangled photons,[46] showing that the addition of $2^N-2$ ancillary photons yields a success rate of $1-1/2^N$. Zaidi and van Loock presented a dual-rail unambiguous BSM scheme by using single-mode squeezers and beam splitters with a success probability of 64.3%.[47] Kwait and Weinfurter first proposed a scheme to perform the complete BSM with linear optics by using entanglement in polarization DOF and ancillary DOF.[48] After that, a series of complete BSM schemes was put forward by using the hyperentangled states, such as hyperentanglement in polarization-momentum,[49] polarization-frequency,[50] and polarization-time mode.[51,52] In these schemes,the quantum message is usually carried by the polarization DOF, while the ancillary DOFs are used to expand the measurement space.

Owing to the above progresses, the practical BSM technology has been greatly developed, while how to distinguish Bell states unambiguously and efficiently in quantum information fields is still a very crucial research topic, and this will also be an important aspect of our future work.

## 6. Conclusions

In this work, we present a multi-particle HSES scheme for the bidirectional teleportation of three-particle GHZ states, in which the intermediate nodes on the quantum path are divided into several segments, and the whole entanglement swapping includes level-one SES and level-two SES. Owing to the fact that the classical information transmission is limited to a smaller scope in level-one SES, and only the intermediate nodes need to transmit classical information to Bob in level-two SES, the classical information cost can be significantly reduced. Compared with the existing SEQES and SES schemes, the HSES has the advantages to obtain the optimal performance tradeoff between the end-to-end delay and the classical information cost.

The HSES scheme in this paper can be easily extended for other quantum communication tasks. Generally, a large scale quantum network is divided into quantum access network (QAN) and quantum core network (QCN). In the QAN, different types of entanglements can be distributed between

the user node and the network edge node according to the requirements of quantum communication tasks, such as W state, GHZ state, cluster state, *etc*. In the QCN, the intermediate nodes only need to prepare and distribute Bell states. Using the HSES scheme, the multi-hop entanglement between remote users can be established with low delay and low classical information cost. Such a scheme is of positive value for improving the quality of large scale quantum networks and promoting the development of practical quantum communication, which will have a potential application prospect in constructing the future quantum land networks and quantum satellite networks.

## References


[1] Bennett C H, Brassard G, Crépeau C, Jozsa R, Peres A and Wootters W K 1993 *Phys. Rev. Lett.* **70** 1895
[2] Zheng Y D, Mao Z and Zhou B 2019 *Chin. Phys. B* **28** 120307
[3] Zhou R G, Chen Q and Hou I 2019 *IEEE Access* **7** 42445
[4] Mattle K, Weinfurter H, Kwiat P G and Zeilinger A 1996 *Phys. Rev. Lett.* **76** 4656
[5] Guo Y, Liu B H, Li C F and Guo G C 2019 *Adv. Quantum Technol.* **2** 1900011
[6] Tian M B and Zhang G F 2018 *Quantum Inf. Process.* **17** 19
[7] Shor P W and Preskill J 2000 *Phys. Rev. Lett.* **85** 441
[8] Cui Z X, Zhong W, Zhou L and Sheng Y B 2019 *Sci. China-Phys. Mech. Astron.* **62** 110311
[9] Du G H, Li H W, Wang Y and Bao W S 2019 *Chin. Phys. B* **28** 090301
[10] Wang C, Deng F G, Li Y S, Liu X S and Long G L 2005 *Phys. Rev. A* **71** 44305
[11] Li J, Zhou Z Y, Wang N, Tian Y, Yang Y G and Zheng Y 2019 *IEEE Access* **7** 43948
[12] Zhou Z R, Sheng Y B, Niu P H, Yin L G, Long G L and Hanzo L 2020 *Sci. China-Phys. Mech. Astron.* **63** 230362
[13] Xu H X 2014 *J. CAEIT* **9** 259 (in Chinese)
[14] Takenaka H, Carrasco-Casado A, Fujiwara M, Kitamura M, Sasaki M and Toyoshima M 2017 *Nat. Photonics.* **11** 502
[15] Ren J G, Xu P, Yong H L, *et al.* 2017 *Nature* **549** 70
[16] Zukowski M, Zeilinger A, Horne M A and Ekert A K 2018 *Quantum Inf. Process.* **17** 19
[17] Cheng S T, Wang C Y and Tao M H 2005 *IEEE J. Sel. Area. Comm* **23** 1424
[18] Zhou X Q, Wu Y W and Zhao H 2011 *Acta Phys. Sin.* **60** 040304 (in Chinese)
[19] Chen P, Cai Y X, Cai X F, Shi L H and Yu X T 2015 *Acta Phys. Sin.* **64** 040301 (in Chinese)
[20] Yu X T, Xu J and Zhang Z C 2012 *Acta Phys. Sin.* **61** 220303 (in Chinese)
[21] Liu X H, Nie M and Pei CX 2013 *Acta Phys. Sin.* **62** 200304 (in Chinese)
[22] Wang K, Yu X T, Lu S L and Gong Y X 2014 *Phys. Rev. A* **89** 022329
[23] Cai R, Yu X T and Zhang Z C 2018 *Int. J. Theor. Phys.* **57** 1723
[24] Gao X Q, Zhang Z C and Sheng B 2018 *J. Mod. Opt.* **65** 1698
[25] Gao X Q, Zhang Z C and Sheng B 2018 *Front. Phys.* **13** 130314
[26] Zou Z Z, Yu X T and Zhang Z C 2018 *Front. Phys.* **13** 130202
[27] Zhang Z H, Wang J W and Sun M 2018 *Int. J. Theor. Phys* **57** 3605
[28] Deng F G, Li CY, Li Y S, Zhou H Y and Wang Y 2005 *Phys. Rev. A* **72** 022338
[29] He X L, Liu M and Yang C P 2015 *Quantum Inf. Process.* **14** 1055
[30] Sun S Y, Li L X and Zhang H S 2020 *Int. J. Theor. Phys.* **59** 1017
[31] Zha X W, Zou Z C, Qi J X and Song H Y 2013 *Int. J. Theor. Phys.* **52** 1740
[32] Yang G, Lian B, Nie M and Jin J 2017 *Chin. Phys. B* **26** 040305
[33] Zhou R G and Zhang Y N 2019 *Int. J. Theor. Phys.* **58** 3594
[34] Hillery M, Bužek V and Berthiaume A 1999 *Phys. Rev. A* **59** 1829
[35] Zhou Y Y, Yu J, Yan Z H, Jia X J, Zhang J, Xie C D and Peng K C 2018 *Phys. Rev. Lett.* **121** 150502
[36] Qin H W and Dai Y W 2017 *Quantum Inf. Process.* **16** 64
[37] Xu G B, Wen Q Y, Gao F and Qin S J 2014 *Quantum Inf. Process.* **13** 2587
[38] Sun Z W, Yu J P and Wang P 2016 *Quantum Inf. Process.* **15** 373
[39] Cai T, Jiang M and Cao G 2018 *Quantum Inf. Process.* **17** 103
[40] Braunstein S L and Mann A 1995 *Phys. Rev. A* **51** R1727
[41] Lütkenhaus N, Calsamiglia J and Suominen K A 1999 *Phys. Rev. A* **59** 3295
[42] Calsamiglia J and Lütkenhaus N 2001 *Appl. Phys. B* **72** 67
[43] Barrett S D, Kok P, Nemoto K, Beausoleil R G, Munro W J and Spiller T P 2005 *Phys. Rev. A* **71** 060302
[44] Sheng Y B, Deng F G and Long G L 2010 *Phys. Rev. A* **82** 032318
[45] Ren B C, Wei H R, Hua M, Li T and Deng F G 2012 *Opt. Express* **20** 24664
[46] Grice W P 2011 *Phys. Rev. A* **84** 042331
[47] Zaidi H A and van Loock P 2013 *Phys. Rev. Lett.* **110** 260501
[48] Kwiat P G and Weinfurter H 1998 *Phys. Rev. A* **58** R2623
[49] Walborn S P, Pádua S and Monken C H 2003 *Phys. Rev. A* **68** 042313
[50] Sheng Y B, Zhou L, Cheng W W, Gong L Y, Wang L and Zhao S M 2013 *Chin. Phys. B* **22** 030314
[51] Schuck C, Huber G, Kurtsiefer C and Weinfurter H 2006 *Phys. Rev. Lett.* **96** 190501
[52] Williams B P, Sadlier R J and Humble T S 2017 *Phys. Rev. Lett.* **118** 050501